Heliyon 9 (2023) e12916

Contents lists available at ScienceDirect

Heliyon

journal homepage: www.cell.com/heliyon

Research article

Circ-ATIC regulates esophageal squamous cell carcinoma growth and metastasis through miR-1294/PBX3 pathway

Qian Zhou [a,1], Chengang Lei [a,1], Fenghe Cui [a], Hao Chen [b], Xianzhao Cao [b,*]

[a] Department of Cardiothoracic Surgery, Jingzhou Central Hospital (Jingzhou Hospital Affiliated to Yangtze University), Jingzhou, 434000, Hubei, PR China

[b] Department of Cardiothoracic Surgery, Sinopharm Dongfeng General Hospital, Hubei University of Medicine, Shiyan, 442008, Hubei, PR China

ARTICLE INFO

Keywords:
Esophageal squamous cell carcinoma
Circ-ATIC
MiR-1294
PBX3

ABSTRACT

Esophageal squamous cell carcinoma (ESCC) is a digestive tract malignancy associated with poor clinical outcome. Growing evidence have elucidated that circular RNAs (circRNAs) play important roles in the pathological process of ESCC. However, the detailed mechanisms how circRNAs modulate the development of ESCC remain largely unknown. Our study aimed to decipher the role and mechanism of circ-ATIC (also termed as circRNA_0058063) in regulating the progression of ESCC. We found that circ-ATIC and its host gene ATIC were significantly increased in ESCC tissues and cells compared with the adjacent noncancerous tissues or normal esophagus epithelial cell. Circ-ATIC knockdown substantially reduced proliferation and the number of invaded ESCC cells and retarded EMT process, reflecting by the decreased N-cadherin and elevated E-cadherin. However, the level of host gene ATIC was not changed under circ-ATIC suppression. It was predicted that circ-ATIC could bind to miR-1294 and serve as a sponge RNA. The luciferase reporter assay and RNA immunoprecipitation (RIP) assay confirmed their relations. MiR-1294 was decreased in ESCC tissues and cells, which was reversely correlated with circ-ATIC level. Furthermore, PBX3 was predicted and proved to be a downstream direct target of miR-1294. PBX3 mRNA and protein were obviously upregulated in ESCC tumor tissues and cells. PBX3 overexpression could reverse the suppressive roles of miR-1294 mimics on ESCC proliferation and invasion. In an xenograft nude mice model, stable transfection of sh-circ-ATIC significantly retarded the growth of tumor and suppressed VEGF and Ki67. Collectively, circ-ATIC promoted ESCC proliferation and invasion by regulating miR-1294/PBX3 axis.

1. Introduction

Esophageal cancers rank eighth among the most frequent malignant cancers in human and represent one of common causes of death around the world [1]. Epidemiological data reveal that the incidence of esophageal cancer is rapidly rising due to chronic and long-term exposure to smoking, alcohol consumption, inappropriate diet intake, environmental pollution, and other harmful stimuli to cause esophageal injuries [2]. Esophageal cancers are mainly comprised of esophageal squamous cell carcinoma (ESCC) and esophageal adenocarcinoma, with the former histological subtype accounting for up to 90% of all cases worldwide, especially in eastern

* Corresponding author. Department of Cardiothoracic Surgery, Sinopharm Dongfeng General Hospital, Hubei University of Medicine, No. 16 Daling Road, Zhangwan District, Shiyan, 442008, Hubei, PR China.
E-mail address: chaoxianzhaodongf@126.com (X. Cao).

[1] Qian Zhou and Chengang Lei contributed equally to this work.

https://doi.org/10.1016/j.heliyon.2023.e12916
Received 8 October 2022; Received in revised form 8 January 2023; Accepted 9 January 2023
Available online 11 January 2023

Asian [3]. ESCC has a poor prognosis with 5-year survival of 15%–18%, in spite of significant improvement in multidimensional treatments of this cancer [1,4]. The high mortality of ESCC is closely related to local-regional recurrence and/or distant metastasis in the early stages of this disease [4,5]. Therefore, it is of great importance to decipher the mechanism of ESCC metastasis at molecular level.

Circular RNAs (circRNAs) is a new class of small non-coding RNAs that possesses a structure of covalent closed-loop without 5′-cap and 3′poly-A tail formed by means of reverse splicing, which increases the stability of RNA by resisting the hydrolysis of RNase R [6]. CircRNAs are expressed in a cell and tissue-specific manner and play a wide range of roles in various physiological and pathological processes, such as transcriptional and posttranscriptional regulation, chromatin modification and protein encoding [7]. Multiple lines of evidence revealed that exonic circRNAs could serve as sponges to adsorb miRNAs, in turn leading to the functional inhibition of these miRNAs and their relevant targets [8]. Besides, other circRNAs are elucidated to exert their functions by binding to RNA-associated proteins to modulate gene transcription [3]. However, the detailed mechanisms of circRNAs in transcriptional or post-translational regulation are still incompletely unrevealed.

Increasing researches have confirmed that circRNAs, acting as tumor suppressor genes or oncogenes, are involved in the onset and progression of various cancers, including ESCC [7]. CircRNA_0058063 is located at the fragment of chromosome 2: 216177220-216213972 based on the human reference genome (GRCh38.p13) information, and it is derived from the 5-aminoimidazole-4-carboxamide ribonucleotide formyltransferase/IMP cyclohydrolase (ATIC) gene located at chromosome 2q35 [9]. Therefore, circRNA_0058063 is also termed as circ-ATIC. Circ-ATIC was elucidated as an oncogene in bladder cancer by promoting proliferation and invasion of tumor cells [10]. Besides, circ-ATIC dysregulation in ESCC accelerated anaerobic metabolism by promoting glucose uptake via GLUT1 [11]. However, mechanisms how circ-ATIC regulating ESCC metastasis are still poorly understood. Our study aimed to discover roles and mechanisms of circ-ATIC in regulating ESCC proliferation and propagation.

2. Material and methods

2.1. Collection of ESCC samples

ESCC specimens (tumor) and their paired adjacent noncancerous tissues (control) were collected from 36 patients who were admitted to Jingzhou Central Hospital from September 2017 to August 2019. All patients were pathologically diagnosed with ESCC and underwent radical excision without receiving radiotherapy or chemotherapy before surgery. All specimens were immediately frozen in liquid nitrogen after excision and stored at −80 °C. This study was approved by the Institutional Review Board of our hospital. Written informed consents were signed by all patients enrolled in this study.

2.2. Cell culture

A normal immortalized human esophagus epithelial cell line HET-1A was obtained from ScienCell Research Laboratory (Carlsbad, CA, USA). Human ESCC cell lines, KYSE-510 and KYSE-520, were obtained from the Cell Bank of the Chinese Academy of Sciences (Shanghai, China). ESCC cells were grown in Dulbecco's Modified Essential Medium (DMEM) medium (Hyclone, UT, USA) supplemented with 10% fetal bovine serum (FBS) (Gibico, CA, USA) in a 37 °C incubator with 5% CO_2 and 95% humidity. HET-1A cells were cultivated under the same cultural conditions in basal medium along with additives obtained from Lonza/Clonetics Corporation (NJ, USA).

2.3. Oligonucleotides transfection

Circ-ATIC siRNA and the corresponding negative control siRNA (si-NC) were designed and synthesized by GenePharma (Shanghai, China). The siRNA sequence were as followings: si-circ-ATIC#1: GUC UCG AUU UUC CGG AAU AAA UC; si-circ-ATIC#2: UCG AUU UUC CGG AAU AAA UCA; si-NC: CAG AGC TAA AAG GGG AAU AAA UC. The miR-1294 mimic and anti-miR-1294 and their matched negative control were obtained from Invitrogen (CA, USA). To upregulate the expression of PBX3, human PBX3 cDNA was synthesized and inserted into pcDNA3.1 vector (Geneseed Biotech Co, Guangzhou, China). The oligonucleotides or vectors were transfected into KYSE510 and KYSE520 cells at a concentration of 60 nmol/L with the assistance of Lipofectamine 3000 (Invitrogen, CA, USA) based on the manufacturer's protocol. To establish KYSE510 cell line with stable knockdown of circ-ATIC, shRNA against circ-ATIC and negative control gene were synthesized and cloned into lentiviruses vectors (OBiO Technology Corp., Ltd. Shanghai, China) for further cellular transfection.

2.4. RT-PCR

Total RNA was isolated from ESCC or adjacent noncancerous tissues as well as treated cells using TRIzol reagent (Invitrogen, USA) based on the manufacturer's protocol. The purified 2.0 μg RNA from each sample was reverse-transcribed into the first-strand of cDNA using the Prime Script RT reagent Kit (Thermo Fisher). A further amplification reaction was performed using PowerUp SYBR Green Master Mix kit (Takara Bio, Dalian, China) in ABI StepOne Plus facility (Applied Biosystems, CA, USA) to detect the expression of circ-ATIC and PBX3. Primers sequences for circ-ATIC, ATIC and PBX3 are listed below: circ-ATIC: 5′-TAT GAT CCT GTT TGG TGG TCG GCA-3′ (forward), 5′-TGG ACC AAG ATG GGT AGC TTG TGA-3′ (reverse); ATIC: 5′-CAC GCT CGA GTG ACA GTG-3′ (forward), 5′-TCG GAG CTC TGC ATC TCC G-3′ (reverse); PBX3: 5′-CTC CCA AAT TCT GGG GAC ATG-3′ (forward), 5′-ATC CAC CTG TGA CTG CAC ATT

G-3′ (reverse). GAPDH was used as an internal control: 5′-CTC TCT GCT CCT CCT GTT CGA C-3′ (forward), 5′-TGA GCG ATG TGG CTC GGC T-3′ (reverse). The relative expression of each gene was normalized to GAPDH by using the $2^{-\Delta\Delta Ct}$ method in three repetitive experiments.

2.5. RNA stability analysis

KYSE510 and KYSE520 cells were incubated with 2 μg/mL actinomycin D for 18 h, and total RNA was extracted from the two cell lines at 0 h, 6 h, 12 h and 18 h after the treatment, respectively. Then, levels of circ-ATIC and its homologous host gene ATIC were measured using RT-PCR. Besides, 5 μg of total RNA extracted from KYSE510 or KYSE520 cells were incubated with 10 units of RNase R (Geneseed Biotech, Guangzhou, China) for 20 min at 37 °C. Afterwards, circ-ATIC and ATIC levels were determined using RT-PCR.

2.6. CCK8 assay

The viabilities of treated ESCC cells were detected using CCK8 kit obtained from Bimake (Shanghai, China). The treated cells were grown in a 96-well plate at a density of 2×10^3 per well. After incubation for indicated time, the cells were harvested and added with 10 μl CCK8 solution and 90 μl medium in each well and cultured for another 4 h. Afterwards, the absorbance at 450 nm was evaluated in a microplate reader (Thermo Fisher Scientific, MA, USA).

2.7. Cell proliferative ability evaluation using EdU staining

The proliferative activities of ESCC cells were evaluated using a EdU (5-Ethynyl-2′-deoxyuridine) Cell Proliferation Kit (Beyotime, Shanghai, China), which was performed based on a rational that EdU acts as a thymidine analogue that can competitively insert into the replicative DNA and react with Apollo fluorescent dye. Then, the labeled cells were observed under a fluorescence microscope (Olympus, Japan) from five randomly selected fields.

2.8. Cell invasion measurement

Invasive capability of incubated ESCC cells was determined using transwell assay. In brief, a 24-well Boyden chamber (Corning Incorporated, NY, USA) was precoated with Matrigel (Invitrogen), and 600 μl DMEM medium supplemented with 10% FBS were added to the lower chamber of Boyden chamber, while ESCC cells at a density of 1×10^5 in 200 μl serum-free medium were seeded into the upper chamber. The plated cells were incubated for 24 h at 37 °C. The cells retained on the upper surface of the chamber were discarded, while cells penetrated the Matrigel were collected and fixed in 4% paraformaldehyde for 20 min. The fixed cells were stained with 0.1% crystal violet and observed under a light microscope (Olympus, Japan). The invasive cells in each group were determined from five randomly chosen fields in 3 repeated operations.

2.9. Western blot

Total proteins were extracted from cultured cells at 70%–80% confluence, or from ESCC and adjacent noncancerous tissues using RIPA lysis reagent (Invitrogen, USA) and quantified by BCA Protein Assay Kit obtained from Beyotime (Shanghai, China). Afterwards, 30 μg proteins were loaded into and separated by SDS-PAGE, which were then electronically transferred to PVDF membranes (GE Healthcare, NJ, USA). Subsequently, the membranes were blocked with 5% non-fat milk for 1 h at room temperature and then were probed with primary antibodies against PBX3 (1:1000, Abcam, Cambridge, UK), CTIC (1:2000, Abcam), E-cadherin (1:500, Abcam) and N-cadherin (1:500, Abcam) and GAPDH (1:1000, Abcam) overnight at 4 °C. The next day, the resultant membranes were washed with tris-buffered saline and Tween 20 TBST for 3 times and incubated with HRP-conjugated secondary antibodies for 3 h at room temperature. ECL prime Detection Kit (Solarbio, Beijing, China) was used to visualize the protein bands. Protein bands data were analyzed using Image J V1.34 software. The uncropped versions of gels were provided as supplementary file.

2.10. Double luciferase report assay

The targeted combination between circ-ATIC and miR-1294 was confirmed using double luciferase report assay as described [12]. In brief, synthesized sequences of wild-type and mutant circ-ATIC (GenePharma Co., Ltd., Shanghai, China) were cloned into pmiRGLO plasmid (OBiO Technology). Then the constructed circ-ATIC-wt or circ-ATIC-mut vehicles were transfected into KYSE510 or KYSE520 cells together with miR-1294 mimics or miR-NC with the assistance of Lipofectamine 3000 (Invitrogen). After 24 h of incubation, the firefly and Renilla luciferase activities were assessed using the dual-luciferase assay system (Promega, Wisconsin, WI, USA). Similarly, the binding between miR-1294 and PBX3 mRNA was also validated by the double luciferase report assay. The wide type 3′-UTR of PBX3 mRNA and the matched mutated 3′-UTR of PBX3 mRNA were prepared and inserted into the downstream of the pmirGLO vector. For the binding detection, the KYSE510 or KYSE520 cells were transfected with miR-1294 mimics or miR-NC, and were simultaneously transfected with the constructed PBX-3′-UTR-wt or PBX-3′-UTR-mut vectors, respectively. The luciferase activities were determined using the Dual-Luciferase Reporter Assay System (Promega).

2.11. RNA immunoprecipitation (RIP) assay

RIP assays were performed based on the manufacturer's guideline to identify the interaction between circ-ATIC, mir-1494 and PBX3 mRNA. In brief, RIP lysis buffer in EZMagna RIP kit (Merck, Darmstadt, Germany) was used to lyse KYSE510 or KYSE520 cells, and the resultant lysates were incubated with magnetic beads that were pre-labeled with Argonaute 2 (AgO2) or IgG antibodies. After 6 h of reaction, the beads were washed in PBS and digested with protease K to remove proteins. At last, the purified RNA was detected using RT-PCR.

2.12. Tumor cell implantation

Healthy male BALB/c nude mice aged 4–5 weeks were purchased from Beijing Vital River Laboratories (Beijing, China). Before *in vivo* implantation, the constructed lentivirus vectors carrying shRNA against circ-ATIC (sh-circ-ATIC) or negative control (sh-NC) were infected into KYSE-510 cells at MOI 100 and the stably knocked cells were screened using 2 μg/mL puromycin continuously for 14

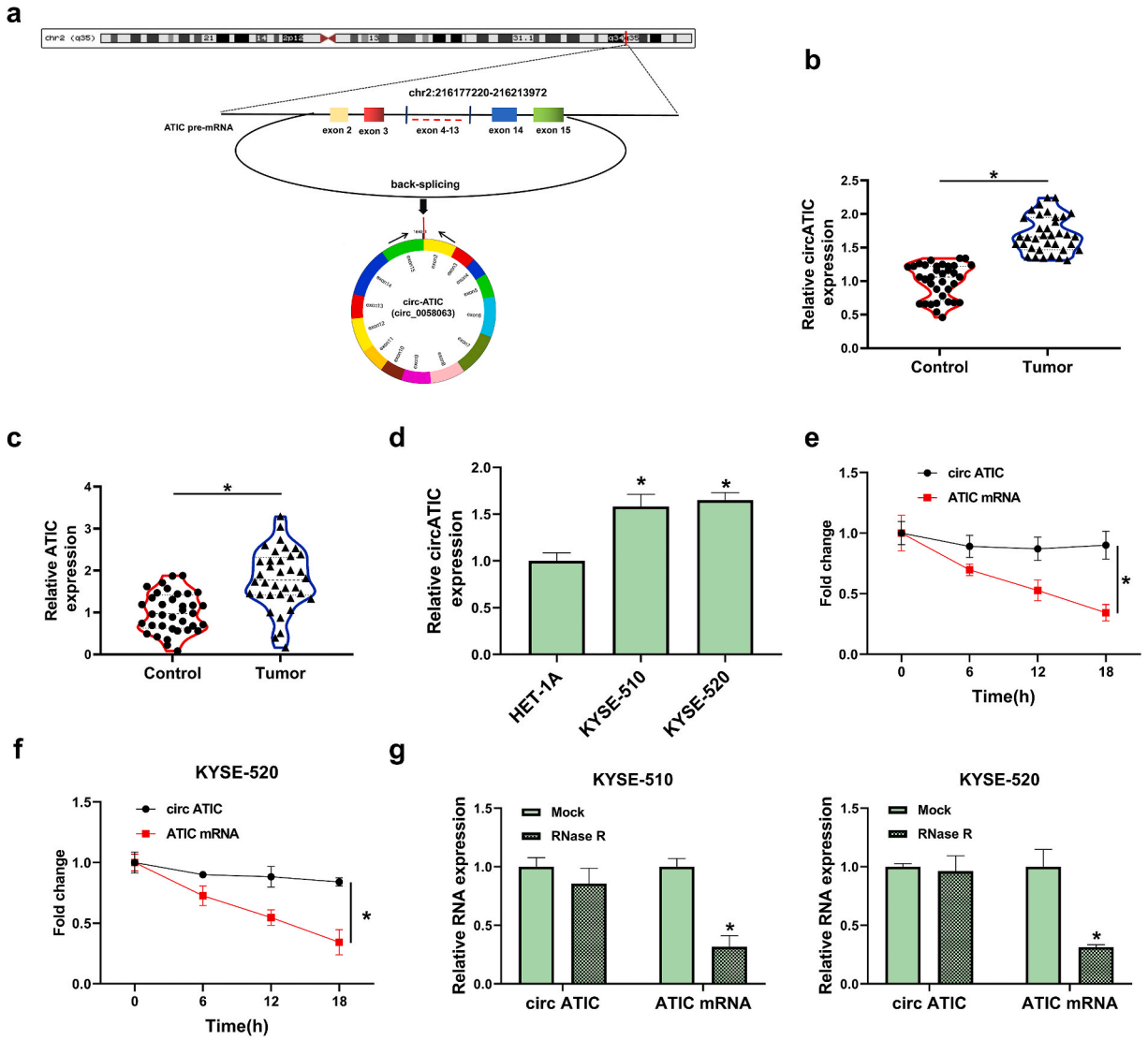

Fig. 1. Expression of circ-ATIC in ESCC tissues and cells and RNA stability. (a) Schematic illustration showing the genomic region of circ-ATIC derived from exons of the ATIC host gene; (b–c) RT-PCR measurement of circ-ATIC and ATIC levels in ESCC tissues (tumor) and the matched adjacent noncancerous tissues (control) (n = 36), *P < 0.05 compared with control; (d) Level of circ-ATIC in normal esophagus epithelial cells (HET-1A) and ESCC cells (KYSE-510 and KYSE-520), *P < 0.05 compared with HET-1A; (e–f) ESCC cells were treated with actinomycin D and the expressions of circ-ATIC and ATIC mRNA were evaluated at indicated time points; (g–h) Total RNA was extracted from ESCC cells and RNase R or vehicle was added, then the remaining circ-ATIC and ATIC mRNA were detected using RT-PCR, *P < 0.05 compared with Mock.

days. Afterwards, 5×10^6 selected cells were subcutaneously injected into the right armpit of nude mice (n = 5 for each group). The length (a) and width (b) of xenografts were measured at a 4 days interval from 7th day after implantation. Volumes of tumors were calculated based on the following formula: volume (mm^3) = $a \cdot b^2/2$ [13]. At day 27th after the operations, all mice were sacrificed under anaesthesia for tumors dissections. The separated tumors were weighted and then snap-frozen or fixed for further histological studies. All animal experiments were approved by Ethics Committee of the Jingzhou Central Hospital and conducted adhering to the guidelines for the ethical review of laboratory animal welfare of China.

2.13. Immunohistochemical staining analysis

The 4% paraformaldehyde fixed tumor tissues were dehydrated in gradient alcohol solutions and embedded in paraffin. Subsequently, the embedded samples were cut into 5 μm specimens, which were deparaffinized, rehydrated and antigens repaired. Following quenching endogenous peroxidase activity using 5% H_2O_2, the sections were blocked with 5% non-fat milk to inhibit non-specific binding. Afterwards, the sections were probed with primary antibodies against VEGF and Ki67 overnight at 4 °C. The next day, the sections were incubated with HRP-connected secondary antibodies for 60 min at 37 °C. The specifically reacted target proteins were then visualized using diaminobenzidine (DAB) and hematoxylin staining. Then the images were taken under microscope at 400 magnifications.

2.14. Statistical analysis

All continuous data were presented as means ± standard deviation (SD) and analyzed by GraphPad Prism 8 and SPSS 24.0 software.

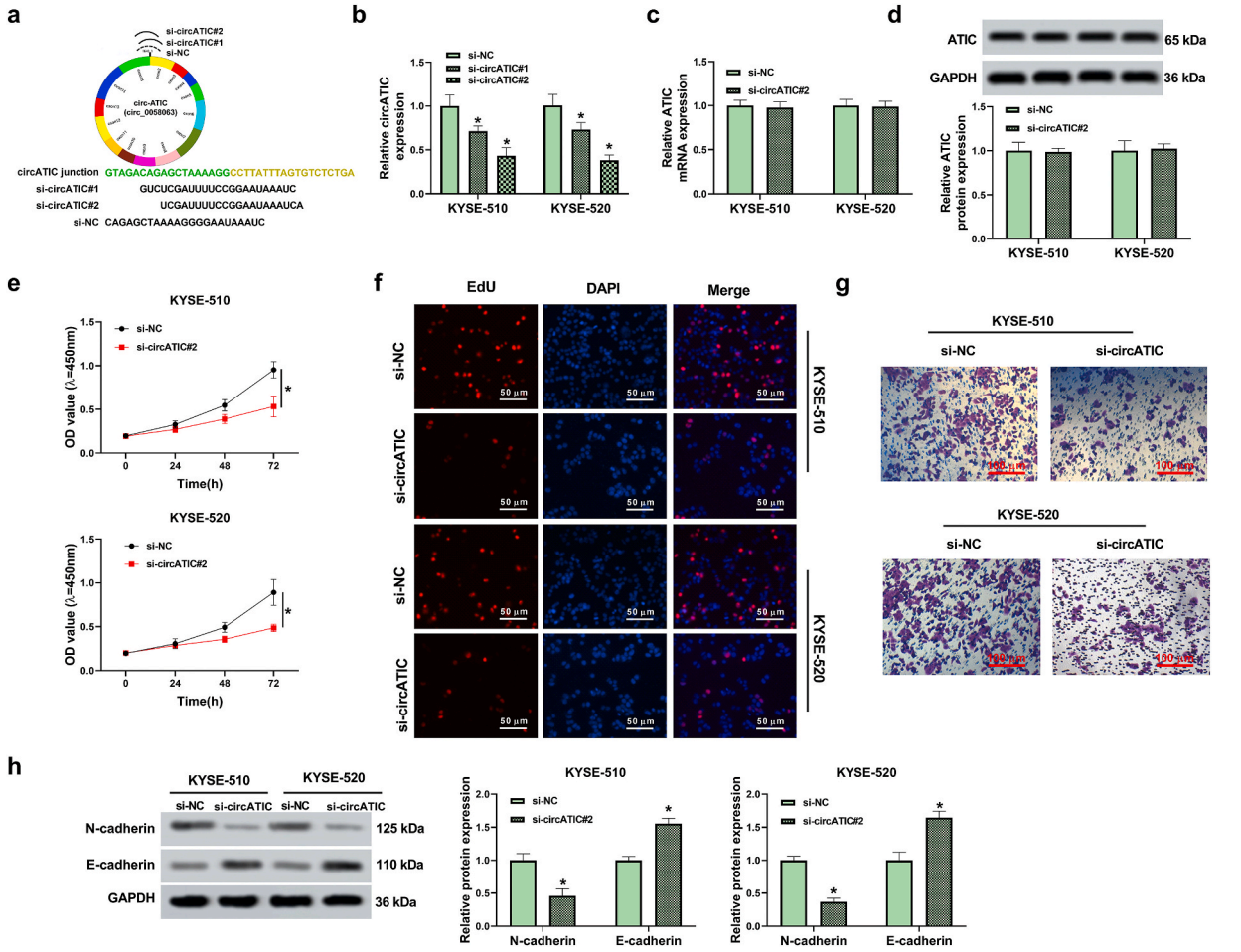

Fig. 2. Circ-ATIC affects proliferation and invasion of ESCC cells. (a) Schematic illustration of the position and sequence of siRNA for circ-ATIC; (b) level of circ-ATIC in ESCC cells after transfection of siRNA or negative control siRNA (si-NC); (c–d) the effect of circ-ATIC interfering on mRNA and protein levels of ATIC; (e) ESCC cellular activity evaluated using CCK8; (f) ESCC cell proliferation detection using EdU staining; (g) Cell invasion after circ-ATIC inhibition was measured using transwell assay; (h) Western blot analysis of N-cadherin and E-cadherin expressions after circ-ATIC siRNA transfection.

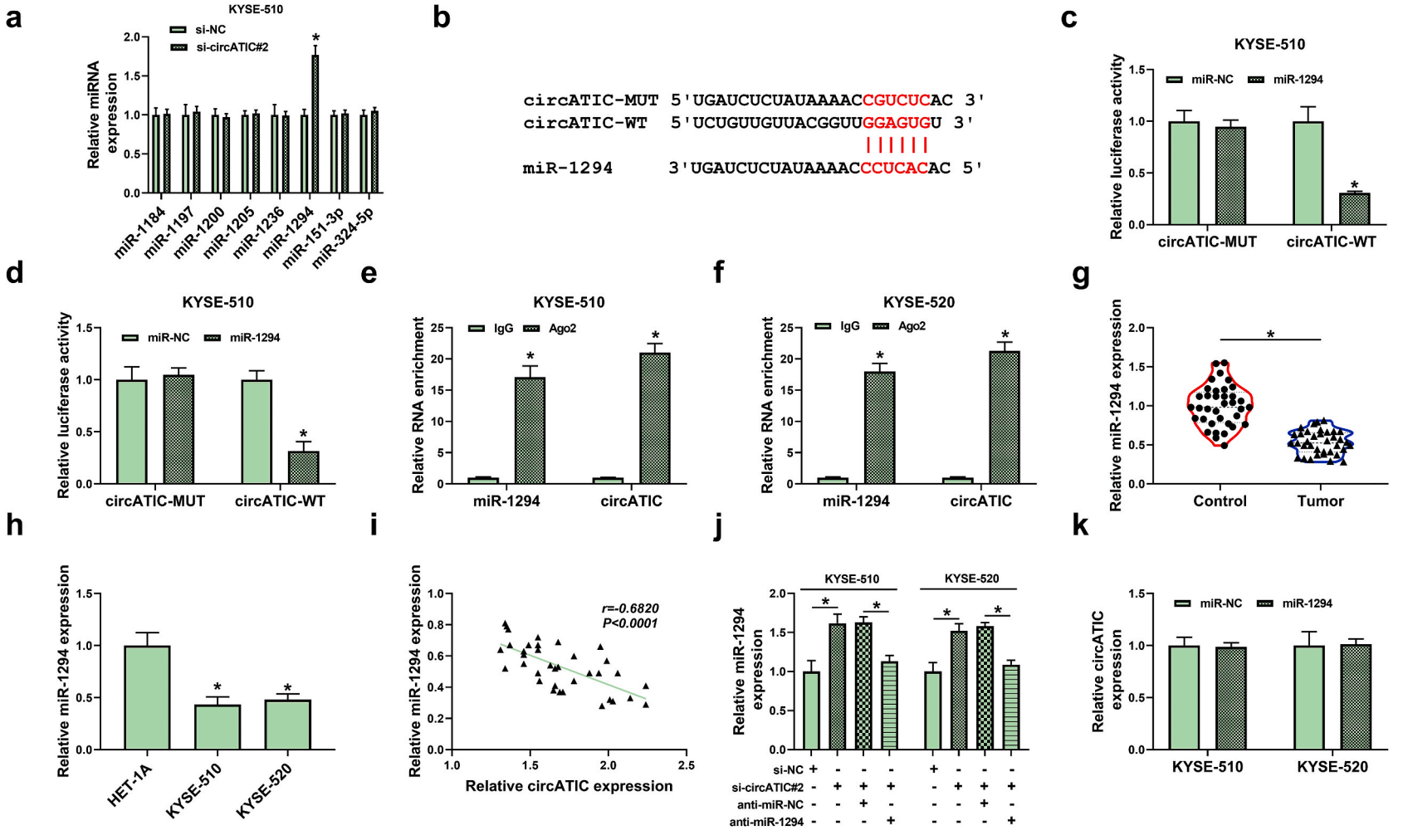

Fig. 3. Circ-ATIC binds to miR-1294 to act as a ceRNA. (a) Eight predicted target miRNA of circ-ATIC were selected and their expressions were assessed in KYSE-510 cell transfected with si-ATIC or si-NC, *P < 0.05 compared to si-NC; (b) the predicted binding sites between circ-ATIC and miR-1294; (c–d) KYSE-510 and KYSE-520 cells were co-transfected with miR-1294 mimic or miR-NC and luciferase reporter plasmids carrying circ-ATIC-wt or circ-ATIC-mut. The relative luciferase activity was detected using dual luciferase reporter system; (e–f) Ago2 RNA immunoprecipitation and RT-PCR assays were performed to analyze the expression of circ-ATIC and miR-1294 in Ago2 immunoprecipitation and IgG immunoprecipitation; (g) miR-1294 level in ESCC tissues and the matched adjacent noncancerous tissues (n = 36), *P < 0.05 compared to normal tissues; (h) level of circ-ATIC in normal esophagus epithelial cells and ESCC cells, *P < 0.05 compared to HET-1A cells. (i) Scattering plot of circ-ATIC and miR-1294 expression in cancer tissues. (j) RT-PCR detection of miR-1294 in KYSE-510 and KYSE-520 cells transfected with si-circ-ATIC and anti-miR-1294, sole or in combination. *P < 0.05; (k) the effect of miR-1294 on circ-ATIC was evaluated in KYSE-510 cell line after overexpressing miR-1294.

Student's t-test was applied to compare the statistical difference between two groups, while one-way ANOVA following by LSD test was used to analyze the difference among three or more groups. The mutual correlations between circ-ATIC, miR-1294 and PBX3 were explored by Pearson's correlation analysis. A P value less than 0.05 was considered statistically significant.

3. Results

3.1. Expression and stability of circ-ATIC in ESCC tissues and cells

Circ-ATIC is located at chromosome 2 and derived from host gene ATIC (Chr 2q35) by back splicing (Fig. 1a). The expression of circ-ATIC and ATIC in 36 ESCC tissue samples and the matched adjacent noncancerous tissues were evaluated using RT-PCR. The results revealed that ESCC tissues presented higher levels of circ-ATIC and ATIC in comparison with the corresponding noncancerous tissues

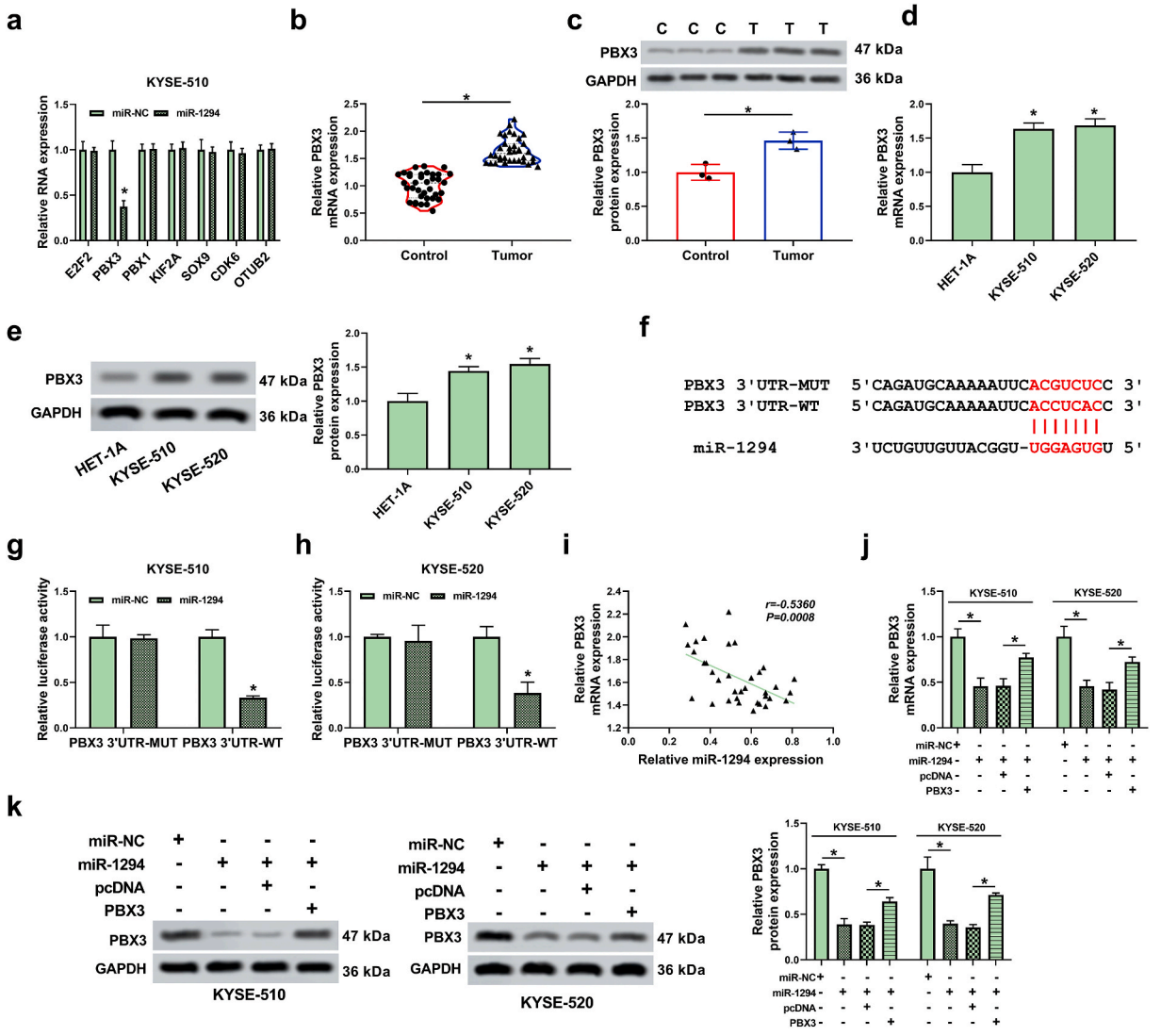

Fig. 4. MiR-1294 directly targets to PBX3 mRNA in ESCC cells. (a) Seven predicted target genes of miR-1294 were selected and their expressions were assessed in KYSE-510 cell transfected with miR-1294 or miR-NC, *P < 0.05 compared to miR-NC; (b) RT-PCR measurement of PBX3 mRNA in ESCC tumor tissues and adjacent noncancerous tissues (n = 36); (c) three representative western blotting images and quantitative results of PBX3 in tumor tissues and adjacent noncancerous tissues of ESCC patients; (d–e) mRNA and protein levels of PBX3 in tumor cell lines and normal cells; (f) the diagram showed the binding sites between PBX3 mRNA 3′-UTR and miR-1294; (g–h) KYSE-510 and KYSE-520 cells were co-transfected with miR-1294 mimic or miR-NC and luciferase reporter plasmids carrying PBX3 3′-UTR-wt or PBX3 3′-UTR-mut. The relative luciferase activity was detected using dual luciferase reporter system; (i) scattering plot of miR-1294 and PBX3 mRNA expressions in cancer tissues; (j–k) RT-PCR and Western blot analysis of PBX3 expression in KYSE-510 and KYSE-520 cells transfected with miR-1294 mimics, sole or in combination with PBX3 overexpressing plasmid. *P < 0.05.

($P < 0.05$) (Fig. 1b and c). Likewise, ESCC cells (KYSE-510 and KYSE-520) expressed higher amount of circ-ATIC compared with the normal esophagus epithelial cell (HET-1A) ($P < 0.05$) (Fig. 1d). Moreover, stability of circ-ATIC and its endogenous host linear gene ATIC in ESCC cells were detected by incubating the cells with actinomycin D, which was a chemical agent unselectively inhibiting RNA synthesis. The RT-PCR experiments suggested that circ-ATIC experienced a slow degradation and only less than 10% of them were lost after 18 h of treatment in the two cell lines. However, more than half of ATIC mRNA was removed from ESCC cells at the termination of the incubation (Fig. 1e and f). Then we assessed the stability of circ-ATIC and ATIC mRNA by treating overall extracted RNA with RNase R, following by RT-PCR measurements. Circ-ATIC had no substantial changes compared with the untreated group. While, ATIC mRNA significantly decreased after being digested with RNase R (Fig. 1g and h).

3.2. Circ-ATIC knockdown inhibits proliferation and invasion of ESCC cells

Two specific siRNAs targeted to different positions of circ-ATIC were constructed and transfected into ESCC cells (Fig. 2a). Both siRNAs showed inhibitory effect on circ-ATIC expression as compared with si-NC, while si-circ-ATIC#2 was more effective (Fig. 2b). Therefore, si-circ-ATIC#2 was used in the following experiments. When knocking out circ-ATIC, mRNA and protein levels of ATIC didn't significantly differ from the negative control, indicating that circ-ATIC may function in other mechanisms (Fig. 2c and d). While circ-ATIC knockdown substantially suppressed the proliferative rate of ESCC cells compared with si-NC group (Fig. 2e). Less EdU positive cells were observed after circ-ATIC silencing compared to the control group (Fig. 2f and g). We also found that the invaded cells reduced in response to circ-ATIC silencing, accompanied by the decrease of N-cadherin and increase of E-cadherin expression (Fig. 2g and h).

3.3. Circ-ATIC binds to miR-1294 and acts as a sponge RNA

The above results demonstrated that elevated circ-ATIC promoted the proliferation and invasion of ESCC cells. However, the underlying mechanism by which circ-ATIC controlled these events remained unrevealed. As most circRNAs functioned as competitive endogenous RNAs (ceRNA) by sponging microRNAs. The potential target miRNAs of circ-ATIC and the binding sites were predicted by online software *circinteractome*. The predicted target miRNAs for circ-AITC were listed (supplementary data 1) and seven interested candidate miRNAs that have been reported functioning in cancers were selected and validated in response to circ-ATIC silencing. As shown in Fig. 3a, only miR-1294 significantly increased when suppressing circ-ATIC. Meanwhile, miR-1294 was confirmed to participate in the progress of ESCC [14]. Therefore, we supposed that circ-ATIC regulated ESCC proliferation and invasion by regulating miR-1294. The predicted binding site between circ-ATIC and miR-1294 was shown in Fig. 3b. To make clear whether circ-ATIC directly interacted with miR-1294, luciferase reporter assay and RNA immunoprecipitation assay were performed. Luciferase reporter activity decreased by more than 50% both in KYSE510 and KYSE520 cells co-transfected with miR-1294 mimics and circ-ATIC-wt plasmid with complete sequence. While miR-1294 mimics did not affect luciferase activity when circ-ATIC sequence were mutated (Fig. 3c–d). Besides, Anti-AgO2 immunoprecipitation assay showed circ-ATIC was significantly enriched in both two cells incubated with Ago2 antibody compared to control IgG immunoprecipitates, suggesting the occupancy of Ago2 in the region of the circ-ATIC (Fig. 3e–f). These data indicated that circ-ATIC functioned as a ceRNA by sponging miR-1294. We further evaluated the level of miR-1294 in ESCC tissues and cells. MiR-1294 was remarkably decreased in tumor tissues and cells compared their corresponding controls ($P < 0.05$) (Fig. 3g–h). A negative correlation was suggested between circ-ATIC and miR-1294 expression in ESCC tissues ($r = -0.682$, $P < 0.001$) (Fig. 3i). Finally, miR-1294 significantly increased in KYSE510 and KYSE520 cells when inhibiting circ-ATIC with siRNA, which were reversed when further treated with anti-miR-1294 (Fig. 3j). When overexpressing miR-1294, the level of circ-ATIC remained unchanged compared with the miR-NC transfected group (Fig. 3k).

3.4. MiR-1294 targets to PBX3 mRNA in ESCC cells

Furthermore, the downstream target genes of miR-1294 was predicted using starbase online software and listed in supplementary excel 2. Seven highly expressed candidate genes of miR-1294 were selected from the list and validated in ESCC cell in the presence of miR-1294 mimics. Pre-B-cell leukemia homeobox 3 (PBX3) was notably suppressed in response to miR-1294 overexpression (Fig. 4a). Previous data showed that PBX3 was a candidate target gene of miR-98 and exerted important functions in mediating tumor growth and propagation in cerebral malignancies [15]. We further detected the expression PBX3 in ESCC tissues and cells using RT-PCR and Western blot. PBX3 mRNA and protein were obviously upregulated both in ESCC tumor tissues and cells comparing with the matched control (Fig. 4b–e). Dual luciferase reporter assay revealed that miR-1294 mimics could bind to the 3′-UTR of PBX3-wt gene rather than the mutated 3′-UTR of PBX3 (Fig. 4f–h). Pearson correlation analysis suggested that miR-1294 was reversely associated with the expression of PBX mRNA ($r = -0.5360$, $P = 0.0008$) in ESCC samples (Fig. 4i). In addition, when miR-1294 was upregulated, the mRNA and protein levels of PBX3 greatly reduced compared the cells transfected with miR-NC. Meanwhile, the suppressive role of miR-1294 on PBX3 was largely reversed by the transfection of PBX3 overexpressing plasmid (Fig. 4j–k).

3.5. MiR-1294/PBX3 regulates proliferative and invasive capabilities of ESCC cells

To investigate the function of miR-1294 and PBX3 in ESCC cell growth and invasion, miR-1294 mimics were introduced to KYSE-510 and KYSE-520 cells alone or in combination with PBX3 overexpressing plasmid. The CCK8 assay demonstrated that compared with miR-NC, cancer cells carrying miR-1294 mimics exhibited significantly decreased cell viability. However, when PBX3 plasmid was

introduced into cells together with miR-1294 mimics, the inhibitory effect of miR-1294 mimics on cell viability was greatly discounted (Fig. 5a–b). Likewise, miR-1294 mimics reduced the EdU positive ESCC cells from 15%–17% to 7%–8%, which were restored by PBX3 overexpression (Fig. 5c–d). The transwell assay revealed that invaded cells reduced by more than 50% in response to miR-1294 upregulation (Fig. 5e–f). MiR-1294 upregulation significantly suppressed the expression of N-cadherin while increased E-cadherin in both two ESCC cells. PBX overexpression further elevated N-cadherin and reduced E-cadherin in ESCC cells treated with miR-1294 mimics (Fig. 5g).

3.6. Circ-ATIC-miR-1294-PBX3 axis affects the growth of ESCC xenografts

To elucidate whether circ-ATIC and miR-1294 functioned upstream to modulate the expression of PBX3, the si-circ-ATIC and anti-

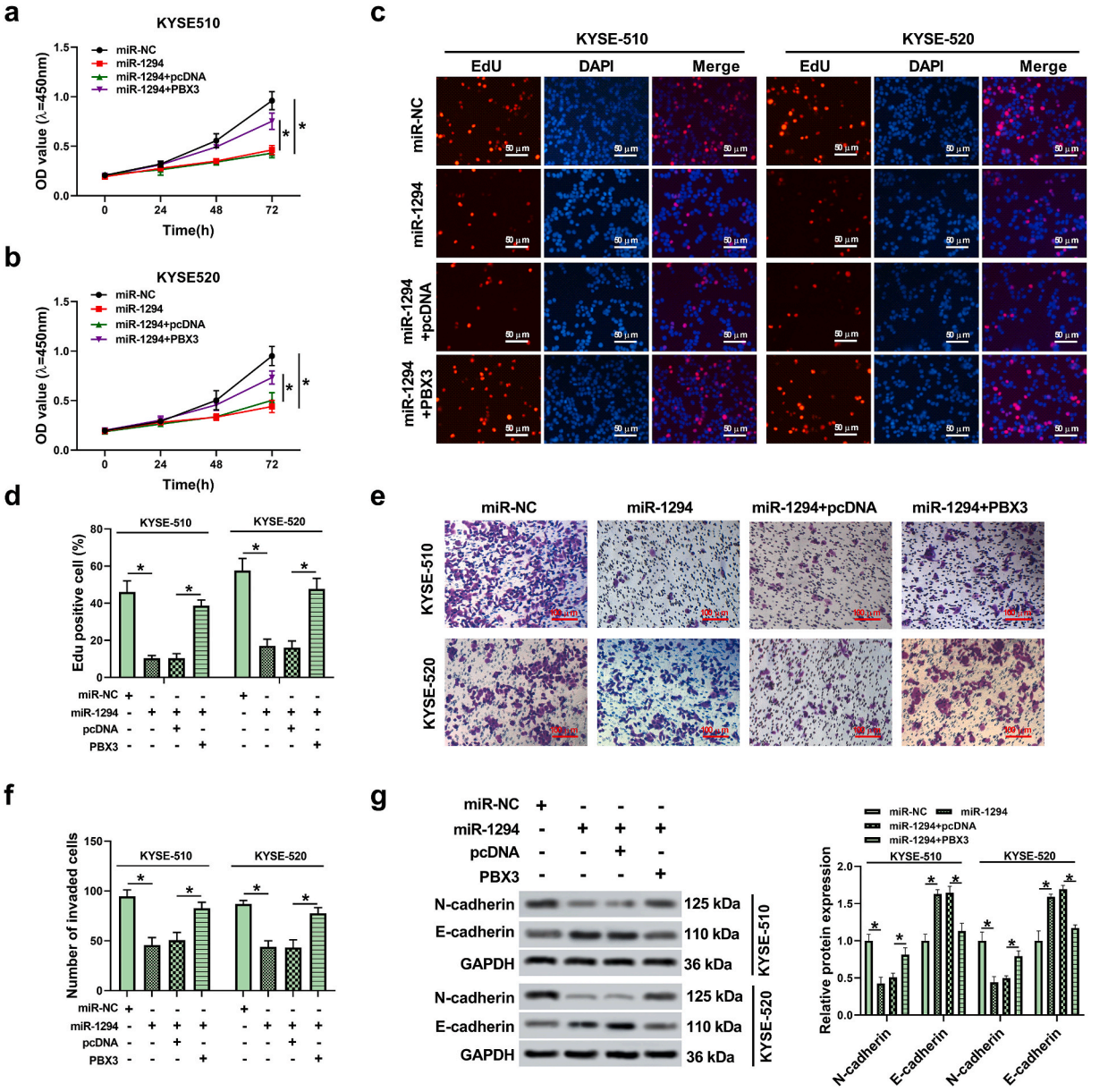

Fig. 5. MiR-1294/PBX3 regulates proliferative and invasive capabilities of ESCC cells. (a–b) MiR-1294 mimics were introduced to KYSE-510 and KYSE-520 cells alone or in combination with PBX3 overexpressing plasmid, cell viability was evaluated at indicated time using CCK8 assay. (c–d) Proliferation of treated ESCC cells was detected using EdU staining and the cells were counted; (e–f) cell invasion capability was measured by transwell assay and number of invaded cells were counted; (g representative Western blot images and quantitative analysis of N-cadherin and E-cadherin expressions after miR-1294 mimic and PBX3 plasmid transfections. *P < 0.05.

miR-1294 oligonucleotides were transfected into ESCC cells. It was found that circ-ATIC inhibition significantly promoted the expression of PBX3. A simultaneously suppression of circ-ATIC and miR-1294 increased PBX3 mRNA and protein compared to that of sole circ-ATIC inhibition (Fig. 6a–b). Since circ-ATIC regulated ESCC progression of ESCC cells *in vitro*, we determined the role of circ-ATIC *in vivo* using an xenograft nude mice model by injecting KYSE510 cells with stable silencing of circ-ATIC or negative control. As shown in Fig. 7a, stable circ-ATIC inhibition significantly retarded the increase of tumor volume. Eventually, the mean tumor weight had a half decrease in sh-circ-ATIC transfection group compared with the control (Fig. 7b). We further assessed the levels of miR-1294 and PBX3. The data showed that antagonizing circ-ATIC expression substantially elevated miR-1294 and reduced PBX3 levels (Fig. 7c–f). IHC staining analysis revealed that less VEGF and Ki67 positive cells accumulated in sections dissected from xenograft transfected with sh-circ-ATIC (Fig. 7g).

4. Discussion

ESCC is one of the most aggressive carcinomas of the gastrointestinal tract and imposes a major ecumenical health quandary [16]. Nowadays, although great development has been achieved in treating ESCC, radical surgery is still the main modality for respectable ESCC. Most ESCC are diagnosed at their middle or advanced stages, and more than half of ESCC patients presented micro-metastases before surgery, which are associated with postoperative metastasis and recurrence of ESCC [17]. Therefore, more studies are required to get deep insight into the mechanisms of the metastasis and recurrence of ESCC.

Metastasis of epithelium-derived cancers, including ESCC, is a multistep process involving roles of various factors and their cross actions [18]. CircRNAs are new subfamily of RNA that exert various functions in a cell type-specific manner. The aberrant circRNAs expression has been implicated in numerous diseases, including ESCC. A more recent study revealed that serum exosomal hsa_circ_0026611 was upregulated in ESCC patients and was associated with lymph node metastasis and poor prognosis of ESCC [19]. Our study found that circ-ATIC (circRNA_0058063) was increased in ESCC cells and tissues, which resulted in elevated cell proliferation and invasion. Circ-ATIC has been proved an oncogene in bladder cancer cells [10]. Meanwhile, circ-ATIC participated in the regulation of anaerobic metabolism in ESCC cells [11]. A more recent study revealed that circ-ATIC was upregulated in ESCC cells and acted as a sponge of miR-326, indicating a complicated network of circ-ATIC in mediating ESCC [20]. Furthermore, as the host gene of circ-ATIC, aberrant ATIC also contributed to the progression of multiple cancers [21]. ATIC is a critical bifunctional enzyme that catalyzes the final 2 steps of the purine *de novo* biosynthetic pathway [22]. Higher ATIC is associated with the progression of several cancers, such as ATIC hepatocellular cancer [23], multiple myeloma tissues [24] and lung adenocarcinoma [25]. It is clarified that ATIC-mediated assembly of the multienzyme purinosome complex is driven by hypoxia via HIF-1 [26]. Our study demonstrated that ATIC was upregulated in ESCC tissues and cells. However, the function of ATIC in ESCC should be further explored. Besides, the potential interaction between circ-ATIC and ATIC in ESCC is another important question needed to be clarified. Currently, the interplay between circRNAs and their host genes are largely unknown. Wang et al. summarized that circRNA regulated the expression and function of host gene in four pathways. It may function as miRNA sponges, regulate transcription and mRNA stability of host genes, and regulate the activity and degradation of parental proteins [27]. We found that modulation of circ-ATIC didn't affect the mRNA and protein level of ATIC, indicating that circ-ATIC play roles in conventional ways via targeting downstream miRNAs.

Generally, expression of circRNAs exhibit spatial and temporal disparities during human development. They exert a wide array of roles in numerous physiological and pathological processes, especially in neutralizing function of microRNA (miRNA) as genomic sponges. Our study confirmed that circ-ATIC could absorb miR-1294 in ESCC cells using dual luciferase reporter system and anti-AgO2 immunoprecipitation assay. MiR-1294 was downregulated in ESCC cells and tissues. Liu et al. found that miR-1294 was downregulated in seventy-nine ESCC patients, and the reduced miR-1294 predicted unfavorable clinical outcome of these patients [14]. Besides, the decreased miR-1294 also contributed the initiation and aggravation of other squamous cell carcinomas, such as laryngeal and oral squamous cell carcinoma [12,28]. Wang et al. found that miR-1294 alleviated EMT procedure via repressing FOXK1 in gastric cancer [29]. It was elucidated that miR-1294 can also be absorbed by LncRNA TUG1 and targeted to PLK in esophageal cancer [30].

Preleukemia transcription factor 3 (PBX3) belongs to the PBX transcription factors family that possess evolutionary conserved

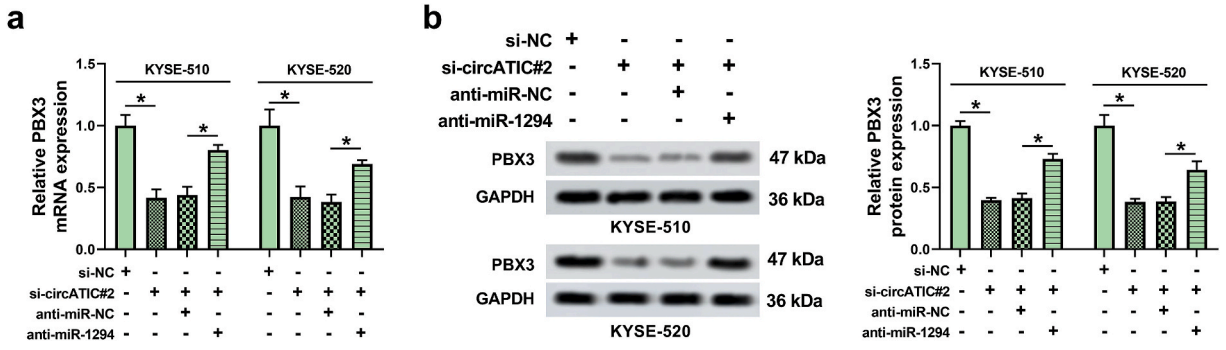

Fig. 6. Circ-ATIC-miR-1294 regulates expression of PBX3. (a–b) si-circ-ATIC was transfected into KYSE510 and KYSE520 cells alone or in combination with miR-1294 inhibitor (anti-miR-1294) for 48 h, the PBX mRNA and protein were detected using RT-PCR and Western blot.

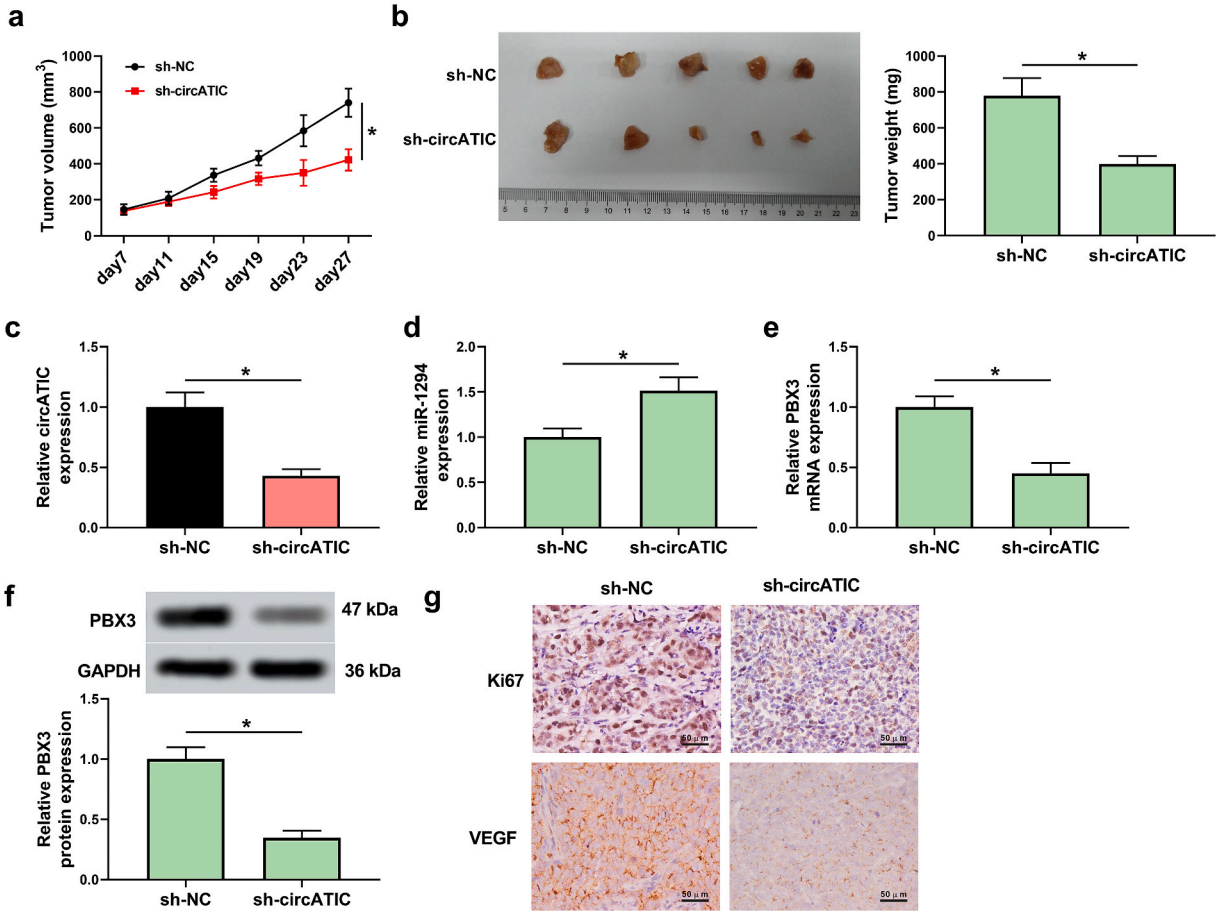

Fig. 7. Circ-ATIC silencing retarded the growth of ESCC xenografts. (a–b) KYSE510 cells with stable transfection of sh-circ-ATIC or sh-NC lentivirus vectors were subcutaneously injected into nude mice (n = 5 per group), the tumor volumes were measured and calculated every four days from day 7 to day 28. After the last assessment, the xenografts were dissected and weighted; (c–d) RT-PCR analysis of circ-ATIC and miR-1294 in xenograft tissues of the two groups of mice; (e–f) RT-PCR and Western blot analysis of PBX3 expression in xenograft tissues; (g) IHC staining of cell proliferative markers VEGF and Ki67 in two groups of xenografts. *P < 0.05 compared with sh-NC.

three-aminoacid-loop-extension (TALE) homeodomain. PBX3 functions as a cofactor for homeobox (HOX) proteins and exhibits pivotal roles in the development and maintenance of malignant phenotype of several human tumors [31]. It is shown that PBX3 has been associated with tumor progression and metastasis in gastric cancer [32]. Besides, PBX3 represents part of EMT regulatory network and promising prognostic predictor for colorectal cancer [33]. We predicted and verified that PBX3 is a downstream target of miR-1294. The reinforced expression of PBX3 is associated with the increased proliferation and invasion capacity of ESCC. Likewise, PBX3 silencing was depicted to restrain ESCC cell progression [34]. Besides, the disruption of PBX-HOX complex by HRX9 exhibited an antitumor phenotype, which may serve as an alternative therapeutic for ESCC [35].

5. Conclusion

Collectively, our study demonstrated that circ-ATIC was upregulated in ESCC tissues and cells, which showed higher stability than its homologous host gene ATIC. The boosted circ-ATIC potentiated tumor cell proliferation, EMT process and invasion. Circ-ATIC could directly sponge miR-1294, and the resultant decreased miR-1294 receded the suppression to its target PBX3, which then aggregated the progression of ESCC. Therefore, circ-ATIC may serve as a promising therapeutic target for ESCC. However, our study proposed one potential mechanism of circ-ATIC, more comprehensive and deep studies on circ-ATIC regulation network are required to decipher functions of circ-ATIC in ESCC.

Ethics approval and consent to participate

This study was approved by the Institutional Review Board of Jingzhou Central Hospital (SYXK(E)2019-0024). Written informed consent was signed by all patients enrolled in this study.

Author contribution statement

Xianzhao Cao: Conceived and designed the experiments; Contributed reagents, materials, analysis tools or data.
Qian Zhou: Performed the experiments; Contributed reagents, materials, analysis tools or data; Wrote the paper.
Chengang Lei: Performed the experiments; Wrote the paper.
Fenghe Cui: Performed the experiments; Analyzed and interpreted the data.
Hao Chen: Analyzed and interpreted the data.

Funding statement

This research did not receive any specific grant from funding agencies in the public, commercial, or not-for-profit sectors.

Data availability statement

The authors do not have permission to share data.

Declaration of interest's statement

The authors declare there are no competing interests.

Abbreviations

ESCC	esophageal squamous cell carcinoma
circRNAs	circular RNAs
RIP	RNA immunoprecipitation
ATIC	5-aminoimidazole-4-carboxamide ribonucleotide formyltransferase/IMP cyclohydrolase
PBX3	Preleukemia transcription factor 3

Appendix B. Supplementary data

Supplementary data related to this article can be found at https://doi.org/10.1016/j.heliyon.2023.e12916.

References

[1] J. Li, Z. Qi, Y.P. Hu, Y.X. Wang, Possible biomarkers for predicting lymph node metastasis of esophageal squamous cell carcinoma: a review, J. Int. Med. Res. 47 (2019) 544–556, https://doi.org/10.1177/0300060518819606.
[2] A. Sanchez-Danes, C. Blanpain, Deciphering the cells of origin of squamous cell carcinomas, Nat. Rev. Cancer 18 (2018) 549–561, https://doi.org/10.1038/s41568-018-0024-5.
[3] X. Hu, D. Wu, X. He, H. Zhao, Z. He, J. Lin, K. Wang, W. Wang, Z. Pan, H. Lin, M. Wang, circGSK3beta promotes metastasis in esophageal squamous cell carcinoma by augmenting beta-catenin signaling, Mol. Cancer 18 (2019) 160, https://doi.org/10.1186/s12943-019-1095-y.
[4] S. Matsuda, H. Kawakubo, A. Okamura, K. Takahashi, T. Toihata, R. Takemura, S. Mayanagi, K. Hirata, T. Irino, Y. Hamamoto, H. Takeuchi, M. Watanabe, Y. Kitagawa, Distribution of residual disease and recurrence patterns in pathological responders after neoadjuvant chemotherapy for esophageal squamous cell carcinoma, Ann. Surg. (2020), https://doi.org/10.1097/SLA.0000000000004436.
[5] Y. Shi, N. Fang, Y. Li, Z. Guo, W. Jiang, Y. He, Z. Ma, Y. Chen, Circular RNA LPAR3 sponges microRNA-198 to facilitate esophageal cancer migration, invasion, and metastasis, Cancer Sci. 111 (2020) 2824–2836, https://doi.org/10.1111/cas.14511.
[6] X. Chen, J. Jiang, Y. Zhao, X. Wang, C. Zhang, L. Zhuan, D. Zhang, Y. Zheng, Circular RNA circNTRK2 facilitates the progression of esophageal squamous cell carcinoma through up-regulating NRIP1 expression via miR-140-3p, J. Exp. Clin. Cancer Res. 39 (2020) 133, https://doi.org/10.1186/s13046-020-01640-9.
[7] Y. Shi, Z. Guo, N. Fang, W. Jiang, Y. Fan, Y. He, Z. Ma, Y. Chen, hsa_circ_0006168 sponges miR-100 and regulates mTOR to promote the proliferation, migration and invasion of esophageal squamous cell carcinoma, Biomed. Pharmacother. 117 (2019), 109151, https://doi.org/10.1016/j.biopha.2019.109151.
[8] Q. Wang, L. Yang, Y. Fan, W. Tang, H. Sun, Z. Xu, J. Zhou, Y. Zhang, B. Zhu, X. Cao, Circ-ZDHHC5 accelerates esophageal squamous cell carcinoma progression in vitro via miR-217/ZEB1 Axis, Front. Cell Dev. Biol. 8 (2020), 570305, https://doi.org/10.3389/fcell.2020.570305.
[9] H. Liang, H. Huang, Y. Li, Y. Lu, T. Ye, CircRNA_0058063 functions as a ceRNA in bladder cancer progression via targeting miR-486-3p/FOXP4 axis, Biosci. Rep. 40 (2020), https://doi.org/10.1042/BSR20193484.
[10] M. Sun, W. Zhao, Z. Chen, M. Li, S. Li, B. Wu, R. Bu, Circ_0058063 regulates CDK6 to promote bladder cancer progression by sponging miR-145-5p, J. Cell. Physiol. 234 (2019) 4812–4824, https://doi.org/10.1002/jcp.27280.
[11] Y. Zheng, Y. Chen, H. Jiang, H. Zhang, H. Wang, J. Xu, Z. Yu, Circ_0058063 upregulates GLUT1 expression and promotes glucose-uptake in esophageal squamous-cell carcinomas, J. Thorac. Dis. 12 (2020) 925–931, https://doi.org/10.21037/jtd.2019.12.57.
[12] T. Yang, S. Li, J. Liu, D. Yin, X. Yang, Q. Tang, S. Wang, Long non-coding RNA KRT16P2/miR-1294/EGFR axis regulates laryngeal squamous cell carcinoma cell aggressiveness, Am. J. Transl. Res. 12 (2020) 2939–2955.
[13] Y.M. Ji, X.F. Zhou, J. Zhang, X. Zheng, S.B. Li, Z.Q. Wei, T. Liu, D.L. Cheng, P. Liu, K. Song, T. Tan, H. Zhu, J.L. Guo, DEPTOR suppresses the progression of esophageal squamous cell carcinoma and predicts poor prognosis, Oncotarget 7 (2016) 14188–14198, https://doi.org/10.18632/oncotarget.7420.
[14] K. Liu, L. Li, A. Rusidanmu, Y. Wang, X. Lv, Down-regulation of MiR-1294 is related to dismal prognosis of patients with esophageal squamous cell carcinoma through elevating C-MYC expression, Cell. Physiol. Biochem. 36 (2015) 100–110, https://doi.org/10.1159/000374056.
[15] X. Xu, Z. Bao, Y. Liu, J. Ji, N. Liu, MicroRNA-98 attenuates cell migration and invasion in glioma by directly targeting pre-B cell leukemia homeobox 3, Cell. Mol. Neurobiol. 37 (2017) 1359–1371, https://doi.org/10.1007/s10571-017-0466-4.

[16] M.K. Kashyap, O. Abdel-Rahman, Expression, regulation and targeting of receptor tyrosine kinases in esophageal squamous cell carcinoma, Mol. Cancer 17 (2018) 54, https://doi.org/10.1186/s12943-018-0790-4.
[17] X.W. Cai, W.W. Yu, W. Yu, Q. Zhang, W. Feng, M.N. Liu, M.H. Sun, J.Q. Xiang, Y.W. Zhang, X.L. Fu, Tissue-based quantitative proteomics to screen and identify the potential biomarkers for early recurrence/metastasis of esophageal squamous cell carcinoma, Cancer Med. 7 (2018) 2504–2517, https://doi.org/10.1002/cam4.1463.
[18] H. Miyata, K. Sugimura, M. Motoori, T. Omori, K. Yamamoto, Y. Yanagimoto, N. Shinno, M. Yasui, H. Takahashi, H. Wada, M. Ohue, M. Yano, Clinical features of metastasis from superficial squamous cell carcinoma of the thoracic esophagus, Surgery 166 (2019) 1033–1040, https://doi.org/10.1016/j.surg.2019.07.022.
[19] S. Liu, Z. Lin, W. Rao, J. Zheng, Q. Xie, Y. Lin, X. Lin, H. Chen, Y. Chen, Z. Hu, Upregulated expression of serum exosomal hsa_circ_0026611 is associated with lymph node metastasis and poor prognosis of esophageal squamous cell carcinoma, J. Cancer 12 (2021) 918–926, https://doi.org/10.7150/jca.50548.
[20] X. Yue, Z. Chen, J. Zhang, C. Huang, S. Zhao, X. Li, Y. Qu, C. Zhang, Extraction, purification, structural features and biological activities of longan fruit pulp (Longyan) polysaccharides: a review, Front. Nutr. 9 (2022), 914679, https://doi.org/10.3389/fnut.2022.914679.
[21] C.K. Heo, H.M. Hwang, W.H. Lim, H.J. Lee, J.S. Yoo, K.J. Lim, E.W. Cho, Cyclic peptide mimotopes for the detection of serum anti-ATIC autoantibody biomarker in hepato-cellular carcinoma, Int. J. Mol. Sci. 21 (2020), https://doi.org/10.3390/ijms21249718.
[22] X. Liu, U.D. Paila, S.N. Teraoka, J.A. Wright, X. Huang, A.R. Quinlan, R.A. Gatti, P. Concannon, Identification of ATIC as a novel target for chemoradiosensitization, Int. J. Radiat. Oncol. Biol. Phys. 100 (2018) 162–173, https://doi.org/10.1016/j.ijrobp.2017.08.033.
[23] H. Zhang, P. Xia, J. Liu, Z. Chen, W. Ma, Y. Yuan, ATIC inhibits autophagy in hepatocellular cancer through the AKT/FOXO3 pathway and serves as a prognostic signature for modeling patient survival, Int. J. Biol. Sci. 17 (2021) 4442–4458, https://doi.org/10.7150/ijbs.65669.
[24] R. Li, G. Chen, Y. Dang, R. He, A. Liu, J. Ma, C. Wang, Upregulation of ATIC in multiple myeloma tissues based on tissue microarray and gene microarrays, Int. J. Lab. Hematol. 43 (2021) 409–417, https://doi.org/10.1111/ijlh.13397.
[25] N. Niu, J. Zeng, X. Ke, W. Zheng, C. Fu, S. Lv, J. Fu, Y. Yu, ATIC facilitates cell growth and migration by upregulating Myc expression in lung adenocarcinoma, Oncol. Lett. 23 (2022) 131, https://doi.org/10.3892/ol.2022.13251.
[26] C. Doigneaux, A.M. Pedley, I.N. Mistry, M. Papayova, S.J. Benkovic, A. Tavassoli, Hypoxia drives the assembly of the multienzyme purinosome complex, J. Biol. Chem. 295 (2020) 9551–9566, https://doi.org/10.1074/jbc.RA119.012175.
[27] X. Wang, H. Li, Y. Lu, L. Cheng, Regulatory effects of circular RNAs on host genes in human cancer, Front. Oncol. 10 (2020), 586163, https://doi.org/10.3389/fonc.2020.586163.
[28] J. Liu, Q. Yang, H. Sun, X. Wang, H. Saiyin, H. Zhang, The circ-AMOTL1/ENO1 Axis implicated in the tumorigenesis of OLP-associated oral squamous cell carcinoma, Cancer Manag. Res. 12 (2020) 7219–7230, https://doi.org/10.2147/CMAR.S251348.
[29] Y. Wang, G. Liu, S. Sun, J. Qin, miR-1294 alleviates epithelial-mesenchymal transition by repressing FOXK1 in gastric cancer, Genes Genomics 42 (2020) 217–224, https://doi.org/10.1007/s13258-019-00899-3.
[30] M. Zong, W. Feng, L. Wan, X. Yu, W. Yu, LncRNA TUG1 promotes esophageal cancer development through regulating PLK1 expression by sponging miR-1294, Biotechnol. Lett. 42 (2020) 2537–2549, https://doi.org/10.1007/s10529-020-02984-0.
[31] R. Morgan, H.S. Pandha, PBX3 in cancer, Cancers 12 (2020), https://doi.org/10.3390/cancers12020431.
[32] S. Wang, C. Li, W. Wang, C. Xing, PBX3 promotes gastric cancer invasion and metastasis by inducing epithelial-mesenchymal transition, Oncol. Lett. 12 (2016) 3485–3491, https://doi.org/10.3892/ol.2016.5305.
[33] S. Lamprecht, M. Kaller, E.M. Schmidt, C. Blaj, T.S. Schiergens, J. Engel, A. Jung, H. Hermeking, T.G.P. Grunewald, T. Kirchner, D. Horst, PBX3 is part of an EMT regulatory network and indicates poor outcome in colorectal cancer, Clin. Cancer Res. 24 (2018) 1974–1986, https://doi.org/10.1158/1078-0432.CCR-17-2572.
[34] D. Wang, D. You, Y. Pan, P. Liu, Downregulation of lncRNA-HEIH curbs esophageal squamous cell carcinoma progression by modulating miR-4458/PBX3, Thorac. Cancer 11 (2020) 1963–1971, https://doi.org/10.1111/1759-7714.13489.
[35] L.Y. Shen, T. Zhou, Y.B. Du, Q. Shi, K.N. Chen, Targeting HOX/PBX dimer formation as a potential therapeutic option in esophageal squamous cell carcinoma, Cancer Sci. 110 (2019) 1735–1745, https://doi.org/10.1111/cas.13993.